ASSESSMENT OF ELECTRON ENERGY DISTRIBUTIONS IN DISCHARGES BY OPTICAL EMISSION SPECTROSCOPY

Dirk Dodt*, Andreas Dinklage*, Rainer Fischer† and Roland Preuss†

*Max-Planck-Institut für Plasmaphysik, EURATOM Association
Wendelsteinstraße 1, 17491 Greifswald, Germany
†Boltzmannstraße 2, 85748 Garching, Germany

Abstract. A procedure for the reconstruction of electron energy distribution functions (EEDF) of low-temperature neon plasmas from optical emission spectroscopy data is presented. A data descriptive model, including the physics of the plasma discharge and the spectroscopic measurement is developed. Particular refinements of the model regarding the apparatus function of the spectrometer and the optical depth of the plasma for light emission with metastable final states are discussed. The effect of uncertainties in the atomic data entering the model is assessed. Maxwellian and Druyvestein parameterizations for the EEDF are employed. Discrepancies of the reconstructed EEDF with results from independent modelling are not within the error bounds of the data descriptive model.

Keywords: ELECTRON ENERGY DISTRIBUTION FUNCTION, OPTICAL EMISSION SPECTROSCOPY, NEON PLASMA, EEDF
PACS: 52.25.Os

INTRODUCTION

Low-temperature plasmas are widely used nowadays, e.g. in industrial production processes or for lighting purposes [1]. The physics of these discharges is determined by the free-electron gas in the plasma, even with ionization degrees as small as $10^{-6}...10^{-5}$ ions per gas atom. The energy dissipation in inelastic collisions and heating processes requires a kinetic description of the electrons that takes into account the strong deviations from thermodynamic equilibrium. This non-equilibrium behaviour manifests in observed electron energy distribution functions (EEDF) that may substantially deviate from the Maxwellian distribution. A description with two-temperature distribution functions, like the Druyvestein distribution, is more appropriate.

Experimentally, EEDFs are usually determined by electrical probe measurements. This approach suffers from the substantial contact of the electrically biased probe with the plasma. Moreover, the spatial resolution of probe measurements is limited because of the formation of sheaths close to the probe. Therefore, a non-invasive assessment of EEDFs is attractive both for the validation of probe measurements and for physical modelling and process control.

The approach presented here aims at an assessment of the EEDF from emission spectroscopy in the optical regime. The approach employs the light emitted from gas atoms (line emission) that are excited by electron collisions. Since the discharges can

be observed with appropriately designed imaging optics, emission spectroscopy may attain high spatial and temporal resolutions [2]. As the deviations from equilibrium distributions occur in the energy range of the inelastic processes, the light emission can be expected to directly reflect this phenomenon.

Therefore, the idea to use emission spectroscopy for EEDF assessments is long standing, see e.g. [3]. First attempts to use this approach were based on line-ratio techniques, mapping the intensities of different spectral lines onto temperatures. For the plasmas under consideration here, however, the line intensity ratios are affected by too many processes to infer the EEDF directly. Therefore, we extend the approach described in Ref. [4]. The data descriptive model is changed to directly model the raw data, rather than the analysis of pre-analyzed line intensities.

The basic idea is to fit the full physical model to a large number of spectral lines rather than inferring information from a few spectral lines as done in previous approaches. The benefit of this method is expected to result from the consistent use of correlations in the data, which are contained in the physical model of the measurement.

DATA MODEL

The data model maps the quantity of interest, the respective parameterization of the EEDF $f_e(E)$ onto a simulation of the measured data (spectrometer pixels). It consists of a chain of different elements, which are summarized in (1), more details about the data model can be found in [5].

$$\underbrace{\underbrace{f_e(E)}_{\text{kinetic theory}} \rightarrow n_i}_{\text{collisional radiative model}} \rightarrow I_{ij} \underbrace{\rightarrow \int_{\text{l.o.s.}} I_{ij}\,dV}_{\text{radiation transport}} \rightarrow L(\lambda) \underbrace{\rightarrow D(\text{Pixel\#})}_{\text{measurement}} \tag{1}$$

The EEDF determines the electron collision rates for the collisional-radiative model (CRM). Representations of EEDFs, derived from hybrid modelling of neon discharges accounting for a kinetic treatment of the electrons [6], [7] are considered for benchmarking purposes. The CRM yields the population densities n_i of the excited states of neon. The amount of emitted radiation is described by the *locally emitted power* I_{ij} measured in $\left[\mathrm{W}/(\mathrm{m}^3 \cdot \mathrm{sr})\right]$. It is obtained by multiplication with the inverse lifetime of the excited states (Einstein coefficient for spontaneous emission), the photon energy and division by the full solid angle (4π). The radiation has to pass through the plasma before it leaves the discharge device. The apparent lifetime of the excited states is affected by the transport of photons if the absorber density is high, i.e. for transitions to the ground state of the atom. The description of this opacity gives together with the integration along the line-of-sight of the spectrometer, the *spectral radiance* $L(\lambda)$ as a function of the wavelength λ. The modelling of the actual measurement comprises the translation of $L(\lambda)$ into the detected signals and the mapping of wavelengths to pixel numbers. This requires details on the detector response, which were measured with a standard light source (sensitivity calibration). The calibration of the wavelength mapping is fitted to the data within the reconstruction.

Parameters of the model. In addition to the parameters f_e of the EEDF, a number of parameters $\vec{\eta}$ is used in the data model, which describe one of the following aspects:

- external properties of the discharge experiment and the spectrometric setup
- atomic data needed for the plasma model (e.g. cross section and life times of excited states)

Some of these parameters are not known a priori, or subject to significant uncertainty and are nuisance parameters for the reconstruction of the EEDF. The formalism of Bayesian data analysis is used to treat these parameters in a probabilistic way, allowing to quantify the amount of uncertainty introduced to the resulting EEDF. A list of nuisance parameters and the functional form of their prior information is given in table 1.

In the following subsections, specific examples for nuisance parameters are discussed. First, as a set of experimental nuisance parameters, the apparatus function of the spectrometer is described. Second, the incorporation of radiation trapping by metastable atoms is considered, a detail of the collisional-radiative model, which is not assessed in other publications known to the authors.

TABLE 1. Summary of the Parameters $\vec{\eta}$ used in the forward model of the spectroscopic measurement

Symbol	Parameter Description	remarks, prior
σ_{ij}	Electron impact excitation cross sections	scale varied, Gaussian prior
A_{ij}	Einstein coefficients	value varied, Gaussian prior
D_m	Diffusion constant of metastables	constant
Θ_{ij}	Escape factors of transitions to ground state	constants
Θ_{ij}	Escape factors of transitions to the metastable levels	flat prior for eff. densities
p_{Ne}	Gas pressure	constant
T_{Ne}	gas temperature	constant
r	Diameter of the discharge tube	constant
n_{Duran}	Refractive index of glass	constant
d	thickness of glass	constant
$n_{5si,4di}$	Populations of unmodelled atomic levels	Jeffreys prior
$n_{3si,3p,3d,..}$	radial profile of the excited state densities	constant
λ_0, λ', λ''	Wavelength calibration	flat priors
$C(\lambda)$	Intensity calibration	Gaussian prior

Apparatus Function

The data D_k as function of detector pixel number k are given by

$$D_k = C_k \cdot \sum_{ij} \int L_{ij}(\lambda') f(\lambda - \lambda') d\lambda' + \varepsilon_k \tag{2}$$

where C_k is the sensitivity calibration of each pixel and the spectral radiance of the natural line width has to be convolved with the apparatus function f. The error ε of the data is discussed below. Since the width of the apparatus function is large compared to the natural line broadening, the latter may be neglected. In this case, the contribution to

the spectral radiance of a specific line is given by the apparatus function multiplied with the radiance of the respective transition $\overline{L_{ij}}$. The radiance is obtained by the line-of-sight integration of the locally emitted power $I_{ij}(r)$ according to

$$\overline{L_{ij}} = \frac{1}{4\pi} A'_{ij} \frac{\overline{hc}}{\lambda_{ij}} \int_{-R(h)}^{R(h)} n_i(r) dr \tag{3}$$

where R denotes the plasma boundary being a function of the distance h of the line-of-sight from the center of the plasma in cylindrical symmetry.

In first approximation the apparatus function of a spectrometer using a grating as its dispersive element can be described by a Gaussian function (see Fig. 1). A spline is fitted to the measured line profiles to model the deviance from the Gaussian behavior. For this purpose well separated spectral lines from different wavelengths are shifted and rescaled on top of each other and a smoothing spline is fitted to the sum of all data points.

To take into account the spectral variation of the apparatus function an error is determined from the residuals of the smoothing spline fit.

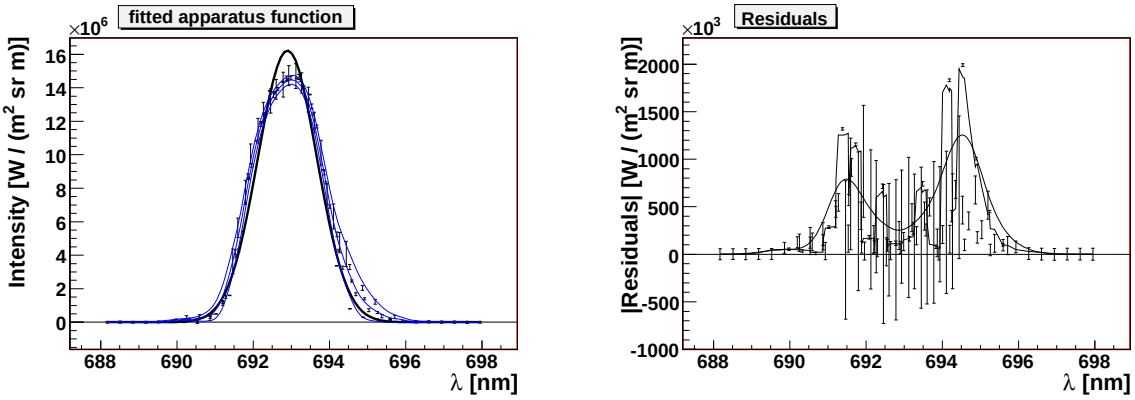

FIGURE 1. Generalized line profile of the spectrometer obtained by shifting and scaling different lines (left, see text). The smoothing spline with the assigned error band is shown together with a Gaussian fit for comparison. The error of the profile is determined using the residuals from the smoothing spline weighted with their respective statistical errors (right)

Optical Depth due to of Metastable Atoms

The light emitted by the excited atoms has to pass through the plasma before it leaves the discharge tube and enters the spectrometer. Atoms in the same atomic state as the emitting atom after its decay may absorb photons. This process leads to an opacity, which is measured by the optical depth for a specific wavelength. The mechanism affects primarily transitions to the ground state causing a higher population density e.g. of the so called resonant states 1s4 and 1s2 (Paschen's notation). In the collisional-radiative model the effect of optical depth is taken into account by considering effective Einstein coefficients $A'_{ij} = \Theta_{ij} A_{ij}$, which contain the *escape factors* $0 < \Theta_{ij} \leq 1$ ($\Theta_{ij} = 1$ meaning no effect of optical depth). Lawler and Curry [8] have published analytic formulas

to obtain approximate escape factors in cylindrical geometry for a constant absorber density. These are used for the transitions to the ground state in our model.

The next highest populated states in the plasma are the metastable levels 1s5 and 1s3 of Neon. Their density is a function of the radial position in the cylindrical discharge tube and it vanishes at the glass walls. The result of Lawler and Curry's approximation which assumes constant absorber density gives a lower limit for the real escape factors for these absorbers. (e.g. transitions to the 1s5 level: Escape Factors have to be greater than ≈ 0.3, which lead to a variation of the modelled spectrum which is greater than the assigned statistical errors.)

To account for the optical depth of the metastable states effective densities are introduced, which are inserted to Lawler and Curry's approximation, instead of the actual population densities from the CRM. These densities are fitted to the spectral data and are expected to be somewhat lower than the population densities at the axis, which are the result of the collisional-radiative model.

DATA ANALYSIS

A Bayesian data analysis is used to find EEDFs leading to results of the data model consistent with the measured data. It is based on a Gaussian likelihood for the modelled intensities and incorporates prior information for nuisance parameters. The error statistics of the spectral measurement, which enter the likelihood described below is dominated by the electronic noise and is considered in Gaussian approximation. Its width is estimated by observing the fluctuations of the spectrometer response with a closed input aperture.

Likelihood. In general the likelihood $P(D|f_e,\vec{\eta},I)$ is the probability to obtain a certain outcome of the measurement D given a set of model parameters describing the EEDF f_e, a set of nuisance parameters $\vec{\eta}$ and other background assumptions I.

Here the probability to measure a pixel intensity D_k given the modelled intensity $D_{k,\mathrm{sim}}(f_e,\vec{\eta})$ is given by the error statistics of the spectroscopic measurement and by the uncertainty of the apparatus function. According to [9] these two sources of uncertainty can be jointly described using a Gaussian likelihood with the effective width of $\sigma_k = \sqrt{\sigma_{k,\mathrm{meas}}^2 + \sigma_{k,\mathrm{app}}^2}$:

$$P(D|f_e,\vec{\eta},I) = \frac{1}{\prod_{k=1}^{N_d}\sqrt{2\pi}\sigma_k}\exp\left\{-\frac{1}{2}\sum_{k=1}^{N_d}\left(\frac{D_k - D_{k,\mathrm{sim}}(f_e,\vec{\eta})}{\sigma_k}\right)^2\right\} \tag{4}$$

Bayesian Data Analysis. Bayes' rule is used to incorporate information which is not contained in the data of the spectroscopic measurement. At the current status of implementation this is used for the nuisance parameters listed in the data model section.

$$P(f_e|D,I) = \int P(D|f_e,\vec{\eta},I)\times\frac{P(f_e,\vec{\eta}|I)}{P(D|I)}\,d\vec{\eta} \tag{5}$$

The Posterior distribution $P(f_e, \vec{\eta}|D,I)$ is a product of the likelihood and the priors $P(f_e, \vec{\eta}|I)$. The $\vec{\eta}$ dependence is marginalized out by integration over $d\vec{\eta}$. The evidence $P(D|I)$ follows from the normalization constraint of the posterior distribution.

Expectation values and variance estimates for the parameters of interest are obtained by sampling the posterior with an implementation of the Metropolis Hastings Monte Carlo algorithm [11]

RESULTS

Figure 2 shows the result of the data model and measured data. The three rows show the spectrum of visible light, from green to near infrared, on a logarithmic scale for the spectral radiance. Almost all spectral features in the considered range are described by the model. For the EEDF reconstruction, a Druyvestein distribution function [10] was used. Figure 3 shows the corresponding result of the EEDF reconstruction. The variance of the reconstruction as obtained by the Monte Carlo method is also displayed. (green error bars, the size of the errors is similar to the width line in the plot and therefore hard to identify.) It incorporates the uncertainties of the spectral measurement, apparatus function and the uncertainty of the wavelength and intensity calibration. Obviously, the variance does not cover the discrepancy to the result from [6], which is shown for comparison. The normalized χ^2/N of the spectrum, that is modelled using a Druyvestein distribution, is $\chi^2/N \approx 7.6$, whereas the best fit Maxwellian distribution gives $\chi^2/N = 10.8$. The resulting electron densities are $n_e^D = (2.1 \pm 0.1) \times 10^{15}\mathrm{m}^{-3}$ and $n_e^M = (7 \pm 0.1) \times 10^{15}\mathrm{m}^{-3}$ for the Druyvestein and the Maxwellian distribution function, respectively. The reference value is $n_e = 2.93 \times 10^{15}\mathrm{m}^{-3}$ [6].

Both the large χ^2/N and the discrepancy of the electron density indicate shortcomings of the model. Nevertheless the Druyvestein distribution, which is closer to the reference distribution, gives a better description of the data and the electron density from [6]. The disagreement within errors with the well validated reference EEDF is taken as an indication, that the uncertainty of the reconstruction is not understood yet. To study this further the uncertainties of the underlying atomic data are addressed.

Influence of Atomic Data

Data for the electron impact excitation are available for Neon from theoretical calculations, e.g. [12]. The overall accuracy of the cross sections in comparison to experimental data is high for the excitation to the lowest excited levels [13] but differs close to threshold energies. The rate coefficient, however, is less affected because of the integration over the energy distribution function.

For a first assessment of the influence of uncertainties in the basis of atomic data, 36 nuisance parameters were introduced varying the scale of the excitation cross sections σ_{ij} of the more prominent processes. Gaussian priors where chosen, with an expectation value of one and a width of 0.25, assigning a 25% relative scale error to the cross sections. With this set of nuisance parameters it is possible to describe the data with an normalized $\chi^2/N \approx 0.8$. The variance propagating onto the reconstruction result (not

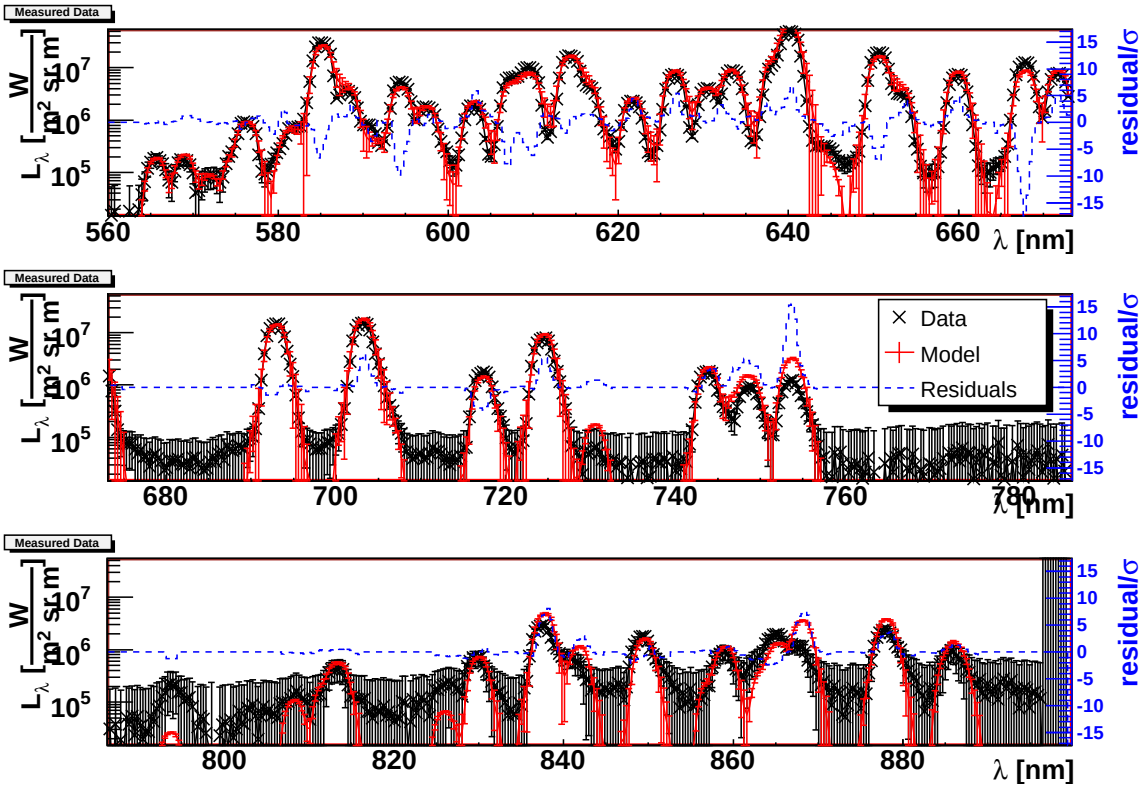

FIGURE 2. Spectral measurement (black crosses) together with the data model (grey/red curve). The parameters of the EEDF are set to their mean expectation values, the uncertainties of atomic data are not taken into account. The error bars correspond to the uncertainties of the measurement and the model (apparatus function). The dashed curve at half height is to be interpreted with the axis on the right hand side and shows the residuals between measurement and model in units of standard deviations. negative residuals correspond to the model having smaller values than the measurement.

shown), however , is comparable to the relative scale error introduced for the cross sections (i.e. 25%). In the plot the error band is still of similar width as the drawn lines. We conclude that the uncertainties considered so far are not able to explain the discrepancy to the EEDF shown for reference.

SUMMARY AND OUTLOOK

A data model for the reconstruction of electron energy distribution functions was set up. The fit of the apparatus function to the data is described. Systematic effects of the optical depth of transitions to the metastable levels were incorporated in the model. First studies of the uncertainties of atomic data do not reveal a satisfactory description of the error band of the reconstruction. The identification of further nuisance parameters and improvements of the model are the next steps. Especially the systematic effects caused by the choice of radial profiles of the excited state densities are to be studied.

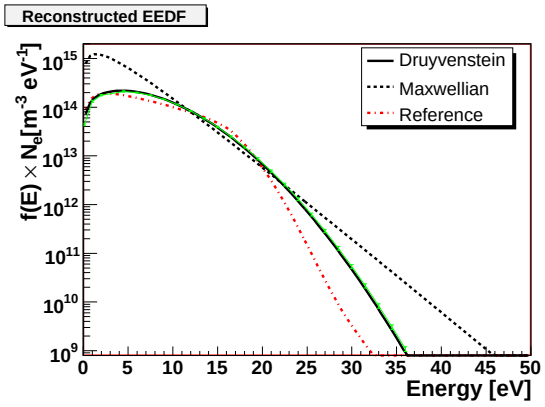

FIGURE 3. The result of the reconstruction is shown for Maxwellian and Druyvestein parameterizations of the EEDF. The dash dotted curve is the well validated result of hybrid modelling of a neon discharge [6], [7] and is shown for comparison. (The discharge parameters are chosen to match the ones of the modelled discharge.)

ACKNOWLEDGMENTS

This work was funded by Deutsche Forschungsgemeinschaft through Sonderforschungsbereich Trans Regio 24 (Fundamentals of Complex Plasmas).

The authors are indebted to V. Dose, H. Dreier, M. Krychowiak, A. Werner, B. Pompe, D. Loffhagen ,F. Sigeneger and D. Uhrlandt for helpful discussions.

REFERENCES

1. J. Meichsner: *Low Temperature Plasmas*. In: *Plasma Physics: Confinement, Transport and Collective Effects*, Springer Lecture Notes Vol. 670, ed. by A. Dinklage et al (Springer, Berlin, 2005)
2. J. Röpcke, P.B. Davies, M. Käning, B.P. Lavrov:: *Diagnostics of non-equilibrium molecular plasmas using emission and absorption spectroscopy*. In: *Low Temperature Plasma Physics*, ed. by R. Hippler et al (VCH-Wiley, Berlin, 2001)
3. N. Brenning, J. Phys. D: Appl. Phys. **15** (1): L1 1982
4. R. Fischer, V. Dose, Plasma Phys. Control. Fusion **41** 1109 (1999)
5. D.Dodt, A. Dinklage, R.Fischer and D. Loffhagen, AIP CP **872** 264 (2006)
6. D. Uhrlandt, St. Franke, J. Phys. D: Appl. Phys. **35**, 680 (2002)
7. S. Franke, diploma thesis *Bilanzgleichungen zur Modellierung der Dynamik einer Neon-Glimmentladung*, Greifswald 1996
8. J. E. Lawler, J. J. Curry, J. Phys. D: Appl. Phys. **31**, 3235 (1998)
9. V. Dose, R. Fischer, and W. von der Linden, edited by G. Erickson, Maximum Entropy and Bayesian Methods, Kluwer Academic, Dordrecht, 147-152 (1998).
10. A. Rutscher *Characteristics of low-temperature plasmas under non-thermal conditions - a short summary*. In: *Low Temperature Plasma Physics*, ed. by R. Hippler et al (VCH-Wiley, Berlin, 2001)
11. Markov chain Monte Carlo in practice, edited by W.R. Gilks, S. Richardson and D.J. Spiegelhalter, Chapmann & Hall, 1996
12. O. Zatsarinny K. Bartschat, J. Phys. B: At. Mol. Opt. Phys. **37**, 2173 (2004)
13. M. Allan, K. Franz, H. Hotop, O. Zatsarinny and K, Bartschat, J. Phys. B: At. Mol. Opt. Phys. **39**, L139 (2006)